Bulletin of Electrical Engineering and Informatics
Vol. 15, No. 6, December 2026, pp. 4825~4836
ISSN: 2302-9285, DOI: 10.11591/eei.v15i6.12094

Investigation of maximum molar point on green hydrogen production using power electronic converter

Ahmad Rosyid Idris[1], Faizal Arya Samman[2], Alamsyah Achmad[1], Musfirah Putri Lukman[1], Syamsumarlin Taha[3]
[1]Department of Electrical Engineering, Faculty of Engineering, State Polytechnic of Ujung Pandang, Makassar, Indonesia
[2]Department of Electrical Engineering, Faculty of Engineering, Hasanuddin University, Makassar, Indonesia
[3]Department of Electrical Engineering, Faculty of Engineering and Informatics, Patria Artha University, Gowa, Indonesia

Article Info

Article history:

Received Dec 10, 2025
Revised Aug 26, 2026
Accepted Sep 12, 2026

Keywords:

Buck converter
Dual-loop control
Green hydrogen production
Maximum molar point
Proton exchange membrane electrolyzer
Renewable-to-hydrogen system

ABSTRACT

Green hydrogen production using photovoltaic (PV)-powered electrolysis is challenged by intermittent irradiance, which changes the electrical operating point of the electrolyzer. This study investigates the maximum molar point (MMP) as a hydrogen-oriented operating concept for a PV–buck–proton exchange membrane (PEM) electrolyzer system. A dual-loop proportional–integral (PI) controller regulates the electrolyzer voltage and current, while the MMP is identified separately through duty cycle characterization. The final model uses one 1Soltech 1STH-220-P PV module and a 50 kHz buck converter. A two-stage duty cycle sweep identifies a near-maximum hydrogen production region at D=0.75–0.85, with approximately 2.537×10^{-5} mol/s at 1,000 W/m². Under irradiance levels from 600 to 1,000 W/m², MMP-oriented operation increases mean hydrogen production by 20.66–73.91% relative to conventional perturb-and-observe (P&O) maximum power point tracking (MPPT). The average hydrogen production rate increases from 1.4386×10^{-5} mol/s for MPPT to 2.2458×10^{-5} mol/s for MMP-oriented operation, corresponding to an average improvement of 55.88%, while the average coefficient of variation (CV) decreases from 0.830% to 0.081%. The results demonstrate the potential of shifting the optimization objective from PV power toward hydrogen production; adaptive online MMP tracking, temperature/degradation effects, and parameter-robustness analysis remain future work.

This is an open access article under the CC BY-SA license.

Corresponding Author:

Ahmad Rosyid Idris
Department of Electrical Engineering, Faculty of Engineering, State Polytechnic of Ujung Pandang
St. Perintis Kemerdekaan Km.10 Tamalanrea, Makassar 90245, Indonesia
Email: ahmadrosyid@poliupg.ac.id

1. INTRODUCTION

The global transition toward decarbonization has strengthened the position of green hydrogen as a clean and sustainable energy carrier for industrial, transportation, and large-scale storage applications [1]–[4]. Green hydrogen can be produced through water electrolysis powered by solar photovoltaic (PV) systems, enabling zero-carbon fuel generation with high scalability and energy density [5]–[7]. However, PV power generation is inherently intermittent due to fluctuating irradiance and temperature, resulting in unstable voltage and current profiles [8], [9]. These fluctuations negatively affect electrolyzer efficiency and accelerate membrane degradation, ultimately reducing hydrogen production yield [10], [11].

To stabilize the power supplied to the electrolyzer, DC-DC converters have been widely used as an electrical interface between PV arrays and hydrogen production systems [10]–[13]. Among various converter

topologies, the buck converter offers high efficiency, simple implementation, and rapid transient response, making it well-suited for renewable-to-hydrogen configurations [14], [15]. However, most previous studies focus on maximizing PV electrical power via maximum power point tracking (MPPT), while overlooking hydrogen molar production. Several recent works reported that the maximum power point (MPP) of PV modules does not always correspond to the operating condition that yields the highest molar hydrogen production [16], [17].

To address this limitation, this study introduces a hydrogen-centric optimization approach. A PV–buck–proton exchange membrane (PEM) electrolyzer system is developed using a dual-loop control strategy to stabilize voltage and current under fluctuating irradiance conditions [18], [19]. Hydrogen production is computed in real-time using Faraday's law, and the maximum molar point (MMP) is defined as the duty cycle operating region that produces the highest molar hydrogen rate.

The contributions of this work can be described in three main aspects. First, an integrated PV–buck–PEM electrolyzer simulation model is formulated with a hydrogen-centric orientation, in which hydrogen molar production becomes the primary optimization target rather than maximizing PV electrical power. Second, a dual-loop control strategy is implemented to improve voltage and current stability during irradiance disturbances, ensuring that the electrolyzer receives a regulated power supply under dynamic solar conditions. Third, a two-stage duty cycle characterization procedure is employed to identify the operating region associated with maximum mean hydrogen production. This MMP identification provides a hydrogen-oriented reference for comparing the proposed operating objective with conventional PV-power-oriented MPPT, without claiming direct adaptive MMP tracking [20], [21].

2. METHOD

This section explains the methodological framework for the proposed PV–buck–PEM electrolyzer system, including system architecture formulation, mathematical modeling, controller design, MMP evaluation, and simulation setup. The methodology is designed to ensure that the simulation reflects real dynamic behavior of PV power and its influence on hydrogen production.

2.1. System architecture

The overall configuration consists of a PV array connected to a buck converter that regulates the power supplied to a PEM electrolyzer. The PV generates DC power as a function of irradiance and temperature, while the buck converter ensures that the electrolyzer receives voltage and current at regulated levels even during power fluctuations [22], [23]. The electrolyzer converts electrical energy to hydrogen according to Faraday's law. Feedback paths from the electrolyzer to the controller ensure that actual voltage and current match their reference values during both steady-state and transient disturbances. The selected architecture prioritizes power conditioning before electrolysis, which has been shown in [24] to improve hydrogen production consistency and membrane durability.

2.2. Mathematical model

2.2.1. Photovoltaic modeling

The PV source is modeled using the MATLAB/Simulink PV array block with the preset 1Soltech 1STH-220-P module. The final configuration contains one module in series and one parallel string. The implemented module parameters are Pmax=218.871 W, Voc=36.6 V, Isc=7.97 A, Vmp=29.3 V, Imp=7.47 A, and 60 cells per module. The single-diode representation is used to reproduce the nonlinear I–V characteristic under irradiance variation [25].

$$I = I_{ph} - I_0(e^{\frac{V+IR_S}{nV_t}} - 1) \quad (1)$$

Where I_{ph} is the photocurrent, I_0 is the diode saturation current, R_s is series resistance, n is diode ideality factor, and V_t is the thermal voltage [25]. This model captures nonlinear I–V behavior under varying irradiance and temperature and ensures realistic power output when subjected to irradiance changes.

2.2.2. Buck converter modeling

The buck converter is described using the averaged state-space:

$$\frac{di_L}{dt} = \frac{1}{L}(D \cdot V_{in} - V_o) \quad (2)$$

$$\frac{dV_o}{dt} = \frac{1}{C}(i_L - \frac{V_o}{R_{load}}) \quad (3)$$

Where D is the duty cycle, i_L is the inductor current, and V_o is the output voltage [14], [26]. This model allows evaluation of transient responses without explicitly simulating high-frequency switching, thereby reducing computational complexity while maintaining accuracy.

Based on the averaged model in (2) and (3), the converter parameters were selected to ensure continuous-conduction operation with limited ripple at the electrolyzer terminals. The inductance L=220 µH and capacitance C=470 µF were sized using the conventional continuous-conduction buck-converter ripple criteria $\Delta IL = (Vin - Vo)D/(Lfs)$ and $\Delta Vo \approx \Delta IL/(8Cfs)$, which provide the engineering basis for limiting inductor-current and output-voltage ripple relative to the electrolyzer operating current and voltage while maintaining stable converter operation. A switching frequency fs=50 kHz (switching period Ts=20 µs) was chosen as a compromise between passive-component size and switching losses, and it lies well above the bandwidth of the voltage and current control loops, which justifies the averaged representation in (2) and (3). The selected values were then verified in the switching simulation under the investigated irradiance range.

2.2.3. Electrolyzer modeling

The PEM electrolyzer voltage is expressed as (4):

$$V_{elec} = E_{rev} + \eta_{act} + \eta_{ohm} + \eta_{conc} \quad (4)$$

where E_{rev} is the reversible voltage and η_{act}, η_{ohm}, and η_{conc} are activation, ohmic, and concentration losses. Hydrogen production follows Faraday's law:

$$\dot{n}_{H_2} = \frac{I}{2F} \quad (5)$$

Where I is the electrolyzer current and F is Faraday's constant [27]. This formulation allows real-time hydrogen estimation directly from simulated current.

It should be noted that the electrolyzer model does not include dynamic temperature variation or long-term degradation. Temperature changes can modify reversible voltage, activation and ohmic losses, and therefore the current–hydrogen relationship at a given converter operating point. Aging of the membrane and electrodes can increase internal resistance and shift the duty cycle region associated with maximum hydrogen production. Consequently, the identified MMP region should be interpreted for the modeled conditions rather than as a lifetime-invariant optimum.

2.3. Dual-loop control strategy

The dual-loop strategy integrates an outer voltage proportional–integral (PI) controller and an inner current PI controller. The outer loop compares the electrolyzer terminal voltage with its reference and generates a current reference, while the inner loop compares this reference with the measured load current and modulates the converter duty cycle. In the final model, the outer PI gains are Kp, v=0.06 and Ki, v=12 with a sampling time of 1 ms; the inner PI gains are Kp, i=0.01 and Ki, i=40 with a sampling time of 20 µs. The gains were obtained through iterative closed-loop tuning in Simulink to achieve stable regulation without sustained oscillation. The faster inner-loop sampling relative to the outer loop preserves the intended cascaded control hierarchy [28]. The nested-loop design is selected because:

- Voltage loop ensures correct operating point of the electrolyzer.
- Current loop ensures fast correction under disturbances.
- The combined structure achieves superior transient stability as demonstrated in [29].

The control objective is not to track the PV MPP, but to maintain the electrolyzer within the optimal hydrogen-producing operating region.

2.4. Maximum molar point evaluation

Conventional MPPT prioritizes maximum PV electrical power, whereas the MMP concept identifies the duty cycle region that produces the highest mean hydrogen molar output. MMP identification was performed in two stages. First, a coarse sweep from D=0.20 to 0.80 with ΔD=0.10 was used to locate the productive duty cycle region. Second, a fine sweep from D=0.55 to 0.85 with ΔD=0.025 was performed around this region. For each duty cycle, the hydrogen molar-flow signal was allowed to reach steady operation and the mean value over the final 20% of the simulation record was used as the evaluation criterion. The duty cycle interval producing the maximum or numerically near-maximum mean hydrogen output was designated as the MMP operating region. This procedure identifies the hydrogen-optimal operating region but does not constitute adaptive online MMP tracking.

It should be emphasized that the MMP procedure employed in this study is an operating-point identification method rather than a fully adaptive MMP tracking algorithm. The duty cycle sweep establishes

the relationship between converter operation and hydrogen molar production and identifies the hydrogen-optimal operating region. The dual-loop voltage–current controller is subsequently used as a baseline regulation structure for operating the system around this region. Therefore, the novelty of the present study lies in establishing and quantitatively evaluating a hydrogen-oriented operating-point framework, while the development of a dedicated adaptive MMP tracking algorithm is reserved for future work.

2.5. Comparative evaluation with maximum power point tracking

To evaluate the hydrogen-oriented operating strategy, a comparative analysis with conventional perturb-and-observe (P&O) MPPT was conducted under identical irradiance, converter, and electrolyzer conditions. The comparison uses mean hydrogen production, standard deviation, coefficient of variation (CV), and percentage improvement at irradiance levels of 600, 700, 800, 900, and 1,000 W/m². These statistics are evaluated over steady-state windows so that switching/start-up transients do not dominate the comparison.

Both operating strategies use the same physical PV–buck–PEM plant model. The numerical benchmark is intentionally limited to P&O MPPT so that the effect of changing the optimization objective—from PV power to hydrogen molar production—can be isolated. More advanced intelligent/adaptive MPPT algorithms are discussed through the literature and reserved for a future like-for-like implementation and tuning study. This evaluation tests whether the PV-power-oriented operating point also maximizes hydrogen molar production and quantifies the difference between the two objectives.

2.6. Simulation setup

All simulations were conducted in MATLAB/Simulink using a 50 kHz switching frequency. The PV model uses one 1Soltech 1STH-220-P module (1 series×1 parallel), the buck converter uses L=220 µH and C=470 µF, and the Faraday efficiency used for hydrogen calculation is ηF=0.965. The tests include steady-state characterization, dynamic irradiance evaluation, duty cycle sweeping for MMP identification, and MPPT–MMP comparison.

- Steady-state condition to examine voltage–current stability and baseline hydrogen production.
- Dynamic irradiance profile to assess disturbance rejection and hydrogen yield robustness during irradiance attenuation.
- Duty cycle sweeping for MMP identification to determine the hydrogen-optimal operating region through a coarse sweep (D=0.20–0.80, ΔD=0.10) followed by a fine sweep (D=0.55–0.85, ΔD=0.025), using the mean hydrogen molar flow over the final 20% of each simulation record as the evaluation criterion.
- MPPT–MMP comparison to evaluate conventional P&O MPPT and MMP-oriented operation under identical plant and irradiance conditions (600–1,000 W/m²) in terms of mean hydrogen production, standard deviation, CV, and percentage improvement.

Model parameters include PV module specification, converter passive elements, control gains, PEM electrolyzer constant values, and Faraday constant. Table 1 summarizes the main simulation parameters for full reproducibility.

Table 1. Simulation parameters

Component	Parameter	Value	Unit
PV module	Model/configuration	1Soltech 1STH-220-P/1S×1P	–
	Rated power (Pmax)	218.871	W
	Voc/Isc	36.6/7.97	V/A
	Vmp/Imp	29.3/7.47	V/A
Buck converter	Inductance (L)	220	µH
	Capacitance (C)	470	µF
	Switching frequency	50	kHz
Control	Outer PI: Kp/Ki/Ts	0.06/12/1	–/–/ms
	Inner PI: Kp/Ki/Ts	0.01/40/20	–/–/µs
Hydrogen model	Faraday efficiency (ηF)	0.965	–
	Faraday constant (F)	96,485.33	C/mol
Irradiance	Evaluation levels	600, 700, 800, 900, 1,000	W/m²

2.7. System control architecture

Figure 1 illustrates the control architecture of the PV–buck–PEM electrolyzer system. The PV source supplies the buck converter, while the dual-loop controller regulates the electrolyzer-side electrical variables through PWM duty cycle control. Hydrogen production is evaluated from the electrolyzer current, and the resulting operating behavior is subsequently used for MMP characterization and comparison with conventional MPPT.

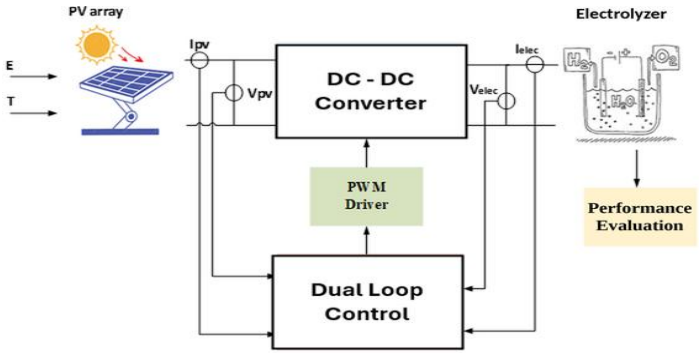


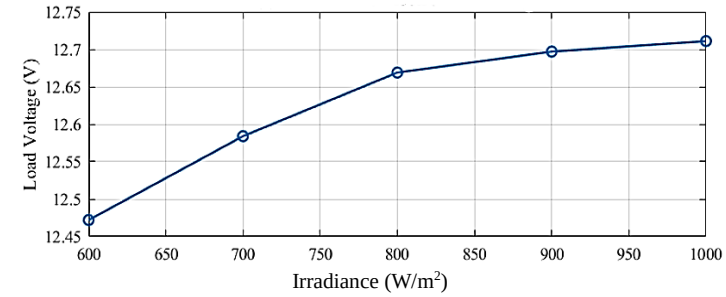
Figure 1. Control architecture of the PV–buck–PEM electrolyzer system

3. RESULTS AND DISCUSSION

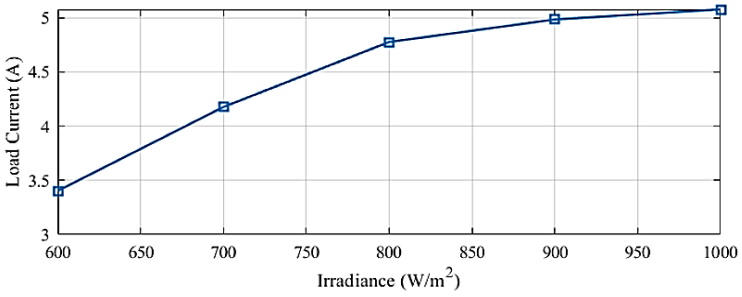
This section presents the steady-state and transient electrical responses, duty cycle characterization for MMP identification, hydrogen production under irradiance variation, and the quantitative comparison between conventional P&O MPPT and MMP-oriented operation.

3.1. Voltage and current stability

Figure 2 presents the steady-state electrical response of the PV–buck–PEM electrolyzer system under irradiance levels ranging from 600 to 1,000 W/m². The regulated load voltage increases moderately from 12.472 V at 600 W/m² to 12.711 V at 1,000 W/m², corresponding to a total variation of only 0.239 V (Figure 2(a)). In contrast, the load current increases from 3.403 A to 5.078 A as the available PV energy increases (Figure 2(b)). These results indicate that irradiance variation is predominantly reflected in the electrolyzer current, while the output voltage remains within a relatively narrow operating range.



(a)



(b)

Figure 2. Steady-state electrical response of the PV–buck–PEM electrolyzer system under different irradiance levels: (a) electrolyzer load voltage and (b) electrolyzer load current

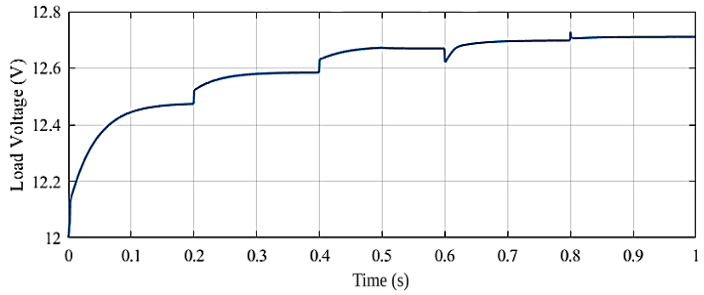
The quantitative steady-state analysis further demonstrates the electrical regulation performance of the dual-loop PI controller. Across the five irradiance levels, the voltage peak-to-peak ripple ranges from 0.001% to 0.036%. The current ripple also remains low, ranging from 0.002% to 0.477%, with the largest value observed at 800 W/m². This regulated electrical behavior is relevant because electrolyzer current directly determines the Faradaic hydrogen production rate.

These results clarify the role of the dual-loop PI structure in the proposed framework. The PI controller provides electrical voltage–current regulation under irradiance variation, whereas the hydrogen-oriented MMP operating region is identified separately through duty cycle characterization, as discussed in subsection 3.3. Therefore, the electrical stability shown in Figure 2 is not interpreted as direct adaptive MMP tracking.

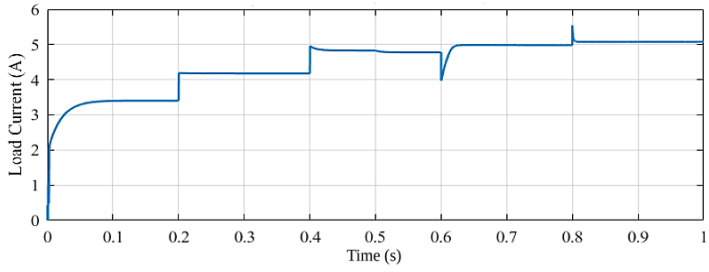
3.2. Dynamic response and transient behavior

Figure 3 shows the dynamic response of the system under the stepwise irradiance profile, where Figure 3(a) presents the electrolyzer load voltage and Figure 3(b) presents the electrolyzer load current. The load voltage in Figure 3(a) follows the changing operating condition smoothly, whereas the load current in Figure 3(b) exhibits larger transient excursions because the available PV power and hydrogen production current change with irradiance. Short deviations occur after the irradiance transitions, particularly around 0.6 and 0.8 s, after which the dual-loop PI controller restores the electrical variables toward their corresponding steady-state values.

Per-step quantitative analysis confirms the transient regulation performance. At the initial 600 W/m² condition, voltage and current settling times are 15.9 and 59.8 ms, respectively. For subsequent transitions, the voltage response remains within the ±2% settling band, while current settling times are 10.7 ms at 800 W/m², 16.2 ms at 900 W/m², and 1.3 ms at 1,000 W/m². Voltage overshoot remains between 0.001% and 0.140%. The largest current overshoot is 9.267% at 1,000 W/m², while steady-state voltage and current ripple remain below 0.036% and 0.477%, respectively. These metrics distinguish the electrical regulation function of the PI loops from the separate hydrogen-oriented MMP identification process.



(a)



(b)

Figure 3. Dynamic response of the PV–buck–PEM electrolyzer system under stepwise irradiance variation: (a) electrolyzer load voltage and (b) electrolyzer load current

As summarized in Table 2, the dual-loop controller maintains stable electrical regulation over the entire irradiance range. The voltage overshoot remains below 0.15%, while the voltage ripple does not exceed 0.036%. The current response exhibits a larger transient deviation, with a maximum overshoot of 9.267% at 1,000 W/m²; however, the steady-state current ripple remains below 0.5% for all operating points. The current settling time is also relatively short after irradiance transitions, reaching 10.7 ms, 16.2 ms, and 1.3 ms at 800, 900, and 1,000 W/m², respectively. These quantitative results complement the waveforms in Figure 3 and confirm that the proposed dual-loop regulation provides a stable electrical interface for the PEM electrolyzer under stepwise irradiance variation.

3.3. Effect of duty cycle on hydrogen production

Figure 4 presents the final fine duty cycle characterization used for MMP identification. The sweep was performed from D=0.55 to 0.85 with a step size of 0.025. The response is non-monotonic below D=0.75

and then forms a near-maximum plateau from approximately D=0.75 to 0.85. The maximum recorded hydrogen production rate is approximately 2.537×10^{-5} mol/s. Therefore, the MMP is reported as an operating region rather than as a single sharp optimum.

The duty cycle characterization establishes the hydrogen-oriented operating region used for comparison with MPPT. Importantly, this is an operating-point identification result: the dual-loop PI controller regulates electrical variables and does not directly use hydrogen molar flow as a feedback signal.

Table 2. Quantitative transient performance under irradiance variation

G (W/m²)	Vss (V)	Iss (A)	Ts,V (ms)	Ts,I (ms)	OS, V (%)	OS, I (%)	Ripple V (%)	Ripple I (%)
600	12.472	3.403	15.9	59.8	0.015	0.001	0.036	0.002
700	12.584	4.177	Within 2%	Within 2%	0.002	0.322	0.006	0.002
800	12.669	4.777	Within 2%	10.7	0.023	3.841	0.001	0.477
900	12.697	4.985	Within 2%	16.2	0.001	0.024	0.003	0.002
1,000	12.711	5.078	Within 2%	1.3	0.140	9.267	0.001	0.003

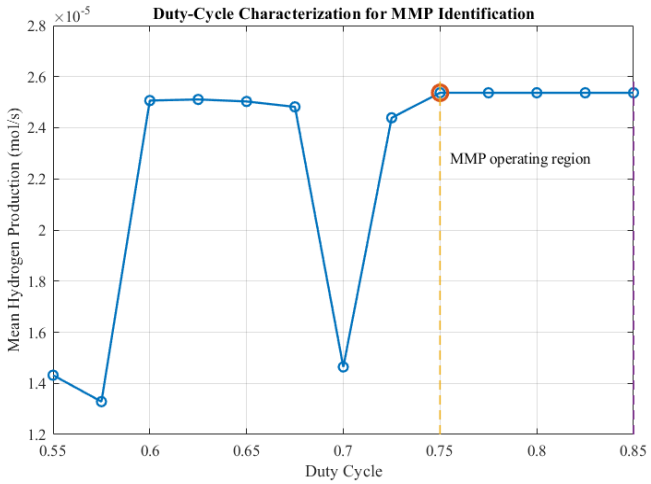


Figure 4. Final duty cycle characterization for MMP identification

3.4. Duty cycle response under irradiance variation

Figure 5 presents the response of the electrical regulation layer under stepwise irradiance variation. Figure 5(a) shows the stepwise irradiance profile from 600 to 1,000 W/m², and Figure 5(b) shows the corresponding duty cycle output of the electrical controller. The duty command rapidly reaches approximately 0.95 and remains nearly constant during the irradiance sequence. Because this value lies outside the MMP region identified in Figure 4, the waveform is presented only as the response of the electrical regulation layer and is not used as evidence of adaptive MMP tracking. This distinction clarifies that the present work identifies the hydrogen-oriented MMP region offline, while online MMP estimation and reference adaptation remain future work.

Accordingly, the dynamic duty cycle response should be interpreted as electrical regulation around a hydrogen-oriented operating condition identified by the preceding sweep. Practical online MMP tracking would require a supervisory mechanism capable of updating the hydrogen-optimal reference as irradiance, temperature, aging, and plant parameters change.

3.5. Hydrogen production under irradiance change

Figure 6 compares the mean hydrogen production rate obtained with conventional P&O MPPT and MMP-oriented operation over irradiance levels from 600 to 1,000 W/m². MMP-oriented operation produces higher mean hydrogen output at every evaluated irradiance level. The advantage increases with irradiance, from 20.66% at 600 W/m² to 73.91% at 1,000 W/m². This result directly addresses the distinction between maximizing PV electrical power and selecting an operating condition based on hydrogen molar production.

Using the final model configuration, the MMP-oriented case yields both higher mean hydrogen production and lower normalized variability over the evaluated steady-state windows. These results support the use of hydrogen production as a system-level optimization objective. Nevertheless, the present implementation should be interpreted as MMP-oriented operating-point selection supported by dual-loop electrical regulation, rather than as a fully adaptive MMP tracking algorithm.

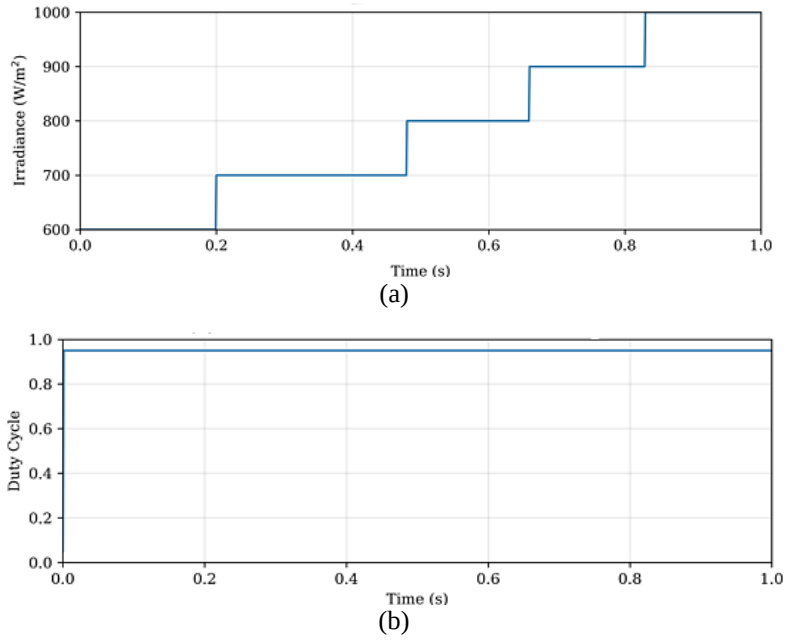


Figure 5. Response of the electrical regulation layer under stepwise irradiance variation, reported as controller behavior rather than direct hydrogen-feedback MMP tracking: (a) irradiance profile and (b) duty cycle output

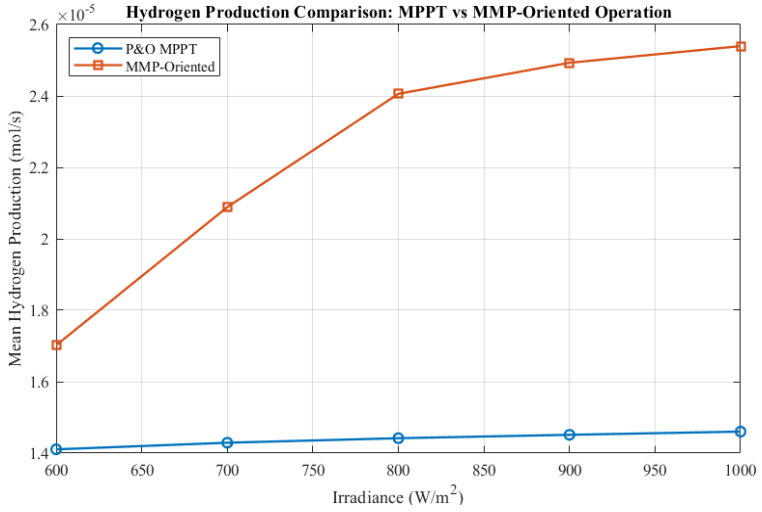


Figure 6. Mean hydrogen production comparison between conventional P&O MPPT and MMP-oriented operation at irradiance levels of 600–1,000 W/m²

3.6. Comparison between maximum power point tracking and maximum molar point

A comparative analysis between conventional P&O MPPT and MMP-oriented operation was conducted under identical plant and irradiance conditions. MPPT adjusts the operating point to maximize PV electrical power, whereas the MMP procedure selects the duty cycle region associated with maximum mean hydrogen molar production. This distinction allows the effect of the optimization objective to be evaluated independently of changes in the physical plant.

The final comparison shows that shifting the objective toward hydrogen production improves the hydrogen-output metric under the investigated conditions. However, the present implementation should still be interpreted as an MMP-oriented operating framework rather than a fully adaptive hydrogen-feedback tracker: the MMP region is identified through duty cycle characterization and the PI loops regulate electrical variables around the selected operating condition.

The quantitative comparison in Table 3 shows that MMP-oriented operation produces higher mean hydrogen output at all five evaluated irradiance levels. Relative to MPPT, the improvement is 20.66% at

600 W/m², 46.15% at 700 W/m², 66.88% at 800 W/m², 71.78% at 900 W/m², and 73.91% at 1,000 W/m². Across all operating points, average hydrogen production increases from 1.4386×10^{-5} mol/s with MPPT to 2.2458×10^{-5} mol/s with MMP-oriented operation, corresponding to an average improvement of 55.88%. The average CV decreases from 0.830% for MPPT to 0.081% for MMP-oriented operation, indicating lower normalized hydrogen-output variability within the evaluated steady-state windows. The CV result is used only as a statistical output-variability metric and is not presented as a substitute for dedicated electrical ripple or converter-efficiency measurements.

These findings clarify both the contribution and its limitation. The present work demonstrates that the hydrogen-oriented objective can select an operating condition that yields more hydrogen than conventional P&O MPPT for the modeled system, but it does not introduce a new adaptive inner-loop control law. In related work, Zou *et al*. [26] used P&O-based PV–electrolysis operation, Mohamed *et al*. [30] investigated alternative MPPT control strategies for PV-powered PEM electrolysis, and Wong and Li [31] compared MPPT and electrolysis-control strategies. Relative to these studies, the present contribution is the explicit duty cycle characterization of a hydrogen-molar objective and its quantitative comparison with PV-power-oriented MPPT. A direct benchmark against advanced intelligent MPPT and an adaptive online MMP supervisor remain future work.

Robustness should also be interpreted within the limits of the present deterministic model. Variations in PV series/shunt resistance, converter L and C, electrolyzer internal resistance, Faraday efficiency, and temperature can alter the electrical operating point and may shift the identified MMP region. No Monte Carlo or formal parameter-sensitivity sweep was performed in this study; therefore, the reported MMP interval is specific to the modeled parameter set. Future work will quantify this uncertainty through parameter sweeps and experimental validation.

Table 3. Quantitative comparison of MPPT and MMP-oriented operation under different irradiance levels

Irradiance (W/m²)	Mean H_2 MPPT (mol/s)	Mean H_2 MMP (mol/s)	Improvement (%)	STD MPPT (mol/s)	STD MMP (mol/s)	CV MPPT/MMP (%)
600	1.411×10^{-5}	1.702×10^{-5}	20.66	8.51×10^{-8}	2.58×10^{-10}	0.604/0.0015
700	1.429×10^{-5}	2.089×10^{-5}	46.15	1.07×10^{-7}	4.33×10^{-10}	0.750/0.0021
800	1.442×10^{-5}	2.406×10^{-5}	66.88	1.23×10^{-7}	9.66×10^{-8}	0.853/0.401
900	1.451×10^{-5}	2.493×10^{-5}	71.78	1.36×10^{-7}	2.77×10^{-10}	0.936/0.0011
1,000	1.460×10^{-5}	2.540×10^{-5}	73.91	1.47×10^{-7}	3.00×10^{-10}	1.006/0.0012
Average	1.439×10^{-5}	2.246×10^{-5}	55.88	—	—	0.830/0.081

4. CONCLUSION

This study investigated a hydrogen-oriented MMP framework for a PV–buck–PEM electrolyzer system. The dual-loop PI structure provides electrical voltage–current regulation, while the MMP is identified separately through duty cycle characterization; therefore, the present PI controller is not claimed to be a direct adaptive hydrogen-feedback MMP tracker.

The two-stage duty cycle sweep identifies a near-maximum hydrogen production region at D=0.75–0.85. The maximum recorded hydrogen production rate is approximately 2.537×10^{-5} mol/s at 1,000 W/m², with the first maximum occurring near D=0.75. Treating this interval as an operating region is more appropriate than claiming a sharp single-point optimum because the response forms a near-maximum plateau.

Under irradiance levels of 600–1,000 W/m², MMP-oriented operation yields higher mean hydrogen production than conventional P&O MPPT at every evaluated level. Average hydrogen production increases from 1.4386×10^{-5} to 2.2458×10^{-5} mol/s, corresponding to an average improvement of 55.88%, while the average CV decreases from 0.830% to 0.081%. The electrical regulator also maintains voltage overshoot below 0.140% and steady-state voltage and current ripple below 0.036% and 0.477%, respectively. These quantitative results demonstrate that maximizing PV electrical power and maximizing hydrogen molar production are distinct objectives while confirming stable electrical operation of the final model.

A limitation of this study is that validation is simulation-based and does not include experimental uncertainty, dynamic temperature effects, long-term electrolyzer degradation, or a formal parameter-sensitivity/Monte Carlo analysis. These effects may change the absolute hydrogen rate and shift the identified MMP region. Although settling time, overshoot, and steady-state ripple have been quantitatively evaluated, converter efficiency has not been reported because semiconductor switching/conduction losses and passive-component losses are not explicitly represented in the present model.

Future work will focus on experimental validation, parameter-sensitivity analysis, and development of an adaptive MMP supervisor that updates the hydrogen-optimal reference online. Temperature and aging effects, partial shading, converter-loss-based efficiency assessment, forecasting-assisted control, hybrid PV–wind supply, and scale-up to larger PV arrays and electrolyzer stacks will also be investigated together with thermal management and power coordination.

ACKNOWLEDGMENTS

The authors express our sincere gratitude to the Ministry of Higher Education, Science, and Technology of the Republic of Indonesia for the financial support that made this research possible. Furthermore, we wish to acknowledge the crucial institutional support received from Politeknik Negeri Ujung Pandang, particularly the Department of Electrical Engineering, for providing access to valuable facilities and resources essential for the successful completion of this work.

FUNDING INFORMATION

Funding for this study was provided by the Ministry of Higher Education, Science, and Technology of the Republic of Indonesia. This support was channeled through the Fundamental Research scheme (Contract No. 29/12/AL.04/2025).

AUTHOR CONTRIBUTIONS STATEMENT

This journal uses the Contributor Roles Taxonomy (CRediT) to recognize individual author contributions, reduce authorship disputes, and facilitate collaboration.

Name of Author	C	M	So	Va	Fo	I	R	D	O	E	Vi	Su	P	Fu
Ahmad Rosyid Idris	✓	✓	✓	✓	✓	✓		✓	✓	✓			✓	
Faizal Arya Samman	✓	✓		✓	✓	✓				✓	✓	✓		
Alamsyah Achmad	✓		✓	✓			✓	✓		✓	✓		✓	✓
Musfirah Putri Lukman		✓	✓		✓		✓			✓		✓		✓
Syamsumarlin Taha				✓		✓		✓		✓	✓	✓	✓	

C : **C**onceptualization
M : **M**ethodology
So : **So**ftware
Va : **Va**lidation
Fo : **Fo**rmal analysis
I : **I**nvestigation
R : **R**esources
D : **D**ata Curation
O : Writing - **O**riginal Draft
E : Writing - Review & **E**diting
Vi : **Vi**sualization
Su : **Su**pervision
P : **P**roject administration
Fu : **Fu**nding acquisition

CONFLICT OF INTEREST STATEMENT

Authors state no conflict of interest.

DATA AVAILABILITY

The data that support the findings of this study are available from the corresponding author upon reasonable request.

REFERENCES

[1] S. Algburi *et al*., "The green hydrogen role in the global energy transformations," *Renewable and Sustainable Energy Transition*, vol. 8, p. 100118, Dec. 2025, doi: 10.1016/j.rset.2025.100118.
[2] H. A. Younus, R. A. Hajri, N. Ahmad, N. Al-Jammal, F. Verpoort, and M. A. Abri, "Green hydrogen production and deployment: opportunities and challenges," *Discover Electrochemistry*, vol. 2, no. 1, p. 32, Aug. 2025, doi: 10.1007/s44373-025-00043-9.
[3] R. Angelico, F. Giametta, B. Bianchi, and P. Catalano, "Green Hydrogen for Energy Transition: A Critical Perspective," *Energies*, vol. 18, no. 2, p. 404, Jan. 2025, doi: 10.3390/en18020404.
[4] D. Guilbert and G. Vitale, "Hydrogen as a Clean and Sustainable Energy Vector for Global Transition from Fossil-Based to Zero-Carbon," *Clean Technologies*, vol. 3, no. 4, pp. 881–909, Dec. 2021, doi: 10.3390/cleantechnol3040051.
[5] A. Ghosh, "Solar-Powered Green Hydrogen from Electrolyzer (PV-H2): A Review," *Solar RRL*, vol. 9, no. 14, Jul. 2025, doi: 10.1002/solr.202500150.
[6] R. S. Nada, M. Emam, and H. Hassan, "Standalone green hydrogen production powered by photovoltaic panels and solar atmospheric water harvesting hybrid system: Experimental investigation," *International Journal of Hydrogen Energy*, vol. 94, pp. 984–996, Dec. 2024, doi: 10.1016/j.ijhydene.2024.11.221.
[7] A. Franco, "Green Hydrogen and the Energy Transition: Hopes, Challenges, and Realistic Opportunities," *Hydrogen (Switzerland)*, vol. 6, no. 2, p. 28, Apr. 2025, doi: 10.3390/hydrogen6020028.
[8] A. Fenniche, A. Harrouz, Y. Bellebna, A. Laidi, and I. Benlaria, "Optimization of hybrid PV-wind systems with MPPT and fuzzy logic-based control," *Indonesian Journal of Electrical Engineering and Computer Science*, vol. 39, no. 2, pp. 747–760, Aug. 2025, doi: 10.11591/ijeecs.v39.i2.pp747-760.
[9] S. J. SeyedShenava, P. Zare, and I. F. Davoudkhani, "Maximizing solar energy harvesting efficiency: Optimal hybrid deep neural learning - based MPPT for Photovoltaic systems under complex partial shading conditions," *Sustainable Computing: Informatics and Systems*, vol. 47, p. 101159, Sep. 2025, doi: 10.1016/j.suscom.2025.101159.
[10] E. Nguyen, P. Olivier, M. C. Pera, E. Pahon, and R. Roche, "Impacts of intermittency on low-temperature electrolysis technologies:

A comprehensive review," *International Journal of Hydrogen Energy*, vol. 70, pp. 474–492, Jun. 2024, doi: 10.1016/j.ijhydene.2024.05.217.
[11] M. Aatabe, W. Jenkal, M. I. Mosaad, and S. A. Hussien, "Stochastic Control for Sustainable Hydrogen Generation in Standalone PV–Battery–PEM Electrolyzer Systems," *Energies*, vol. 18, no. 15, p. 3899, Jul. 2025, doi: 10.3390/en18153899.
[12] C. Zhang *et al.*, "Efficiently coupling water electrolysis with solar PV for green hydrogen production," *Energy Reviews*, vol. 4, no. 3, p. 100151, Sep. 2025, doi: 10.1016/j.enrev.2025.100151.
[13] M. Koundi *et al.*, "Investigation of Hydrogen Production System-Based PEM EL: PEM EL Modeling, DC/DC Power Converter, and Controller Design Approaches," *Clean Technologies*, vol. 5, no. 2, pp. 531–568, Apr. 2023, doi: 10.3390/cleantechnol5020028.
[14] M. E. Şahin, H. I. Okumuş, and M. T. Aydemir, "Implementation of an electrolysis system with DC/DC synchronous buck converter," *International Journal of Hydrogen Energy*, vol. 39, no. 13, pp. 6802–6812, Apr. 2014, doi: 10.1016/j.ijhydene.2014.02.084.
[15] A. A. Hassan, O. Abdel-Rahim, M. Bajaj, and I. Zaitsev, "Power electronics for green hydrogen generation with focus on methods, topologies, and comparative analysis," *Scientific Reports*, vol. 14, no. 1, p. 24767, Oct. 2024, doi: 10.1038/s41598-024-76191-6.
[16] S. Gupta, S. Kalika, and R. C. Luisito, "Maximum power point tracking for solar PV system," *Applied Mechanics and Materials*, vol. 110–116, pp. 2034–2037, 2012, doi: 10.4028/www.scientific.net/AMM.110-116.2034.
[17] M. Y. Worku *et al.*, "A Comprehensive Review of Recent Maximum Power Point Tracking Techniques for Photovoltaic Systems under Partial Shading," *Sustainability (Switzerland)*, vol. 15, no. 14, p. 11132, Jul. 2023, doi: 10.3390/su151411132.
[18] M. Arunachalam and D. S. Han, "Efficient solar-powered PEM electrolysis for sustainable hydrogen production: an integrated approach," *Emergent Materials*, vol. 7, no. 4, pp. 1401–1415, Aug. 2024, doi: 10.1007/s42247-024-00697-y.
[19] R. K. Kumar and P. Samuel, "Designing a hydrogen generation system through PEM water electrolysis with the capability to adjust fast fluctuations in photovoltaic power," *International Journal of Hydrogen Energy*, vol. 82, pp. 1–10, Sep. 2024, doi: 10.1016/j.ijhydene.2024.07.376.
[20] M. Benghanem *et al.*, "Hydrogen Production Methods Based on Solar and Wind Energy: A Review," *Energies*, vol. 16, no. 2, p. 757, Jan. 2023, doi: 10.3390/en16020757.
[21] H. Alhusseini, L. M. Abdali, H. A. Issa, and V. I. Velkin, "Adaptive particle swarm optimization based model predictive control MPPT algorithm for PV systems under partial shading conditions," *Results in Engineering*, vol. 28, p. 107419, Dec. 2025, doi: 10.1016/j.rineng.2025.107419.
[22] P. A. Sesotyo, L. O. M. Idris, T. D. Cahyono, and E. Sadewa, "Evaluating of DC-DC Buck-Boost Converter implementation for Integrated Solar Photovoltaic and Thermoelectric Cooler System," *International Journal of Engineering Continuity*, vol. 4, no. 1, pp. 140–172, Jun. 2025, doi: 10.58291/ijec.v4i1.372.
[23] S. A. Khan, "Improving Solar PV System Performance with DC-DC Converters with MPPT Technique in Real-Time Simulation," *Journal of Electrical Systems*, vol. 20, no. 10s, pp. 8262–8274, Nov. 2024, doi: 10.52783/jes.7099.
[24] S. Mtolo, E. K. Tetteh, N. H. Mthombeni, K. Moloi, and S. Rathilal, "Optimization of Green Hydrogen Production via Direct Seawater Electrolysis Powered by Hybrid PV-Wind Energy: Response Surface Methodology," *Energies*, vol. 18, no. 19, p. 5328, Oct. 2025, doi: 10.3390/en18195328.
[25] M. Khalis, R. Masrour, Y. Mir, and M. Zazoui, "Impact of the saturation current IS and ideality factor N on the performance of the characteristic (I-V) of a solar cell," *Computer Methods in Materials Science*, vol. 19, no. 4, pp. 163–169, 2019, doi: 10.7494/cmms.2019.4.0646.
[26] L. Zou, Q. Shen, G. Yang, S. Li, and N. Huang, "Improved hydrogen production efficiency of a Photovoltaic-Electrolysis system with P&O Algorithm: A case study," *Chemical Physics Letters*, vol. 832, p. 140891, Dec. 2023, doi: 10.1016/j.cplett.2023.140891.
[27] M. Awad, M. M. Mahmoud, Z. M. S. Elbarbary, L. M. Ali, S. N. Fahmy, and A. I. Omar, "Design and analysis of photovoltaic/wind operations at MPPT for hydrogen production using a PEM electrolyzer: Towards innovations in green technology," *PLoS ONE*, vol. 18, no. 7 July, p. e0287772, Jul. 2023, doi: 10.1371/journal.pone.0287772.
[28] T. L. Le, L. V. Truc, and T. N. Tien, "Cascaded PI-Controlled Multistage Boost Converter for Low-Voltage Renewable Sources," *Engineering, Technology and Applied Science Research*, vol. 15, no. 5, pp. 26777–26782, Oct. 2025, doi: 10.48084/etasr.12941.
[29] A. Poulose and S. Kim, "Transient Stability Analysis and Enhancement Techniques of Renewable-Rich Power Grids," *Energies*, vol. 16, no. 5, p. 2495, Mar. 2023, doi: 10.3390/en16052495.
[30] A. A. Mohamed, M. H. Ali, A. I. Omar, and M. Mehanna, "Optimizing green hydrogen production: a comparative analysis of MPPT control strategies for PV-powered PEM electrolyzers using differentiated creative search optimization algorithm," *Scientific Reports*, vol. 16, no. 1, p. 15176, May 2026, doi: 10.1038/s41598-026-46999-5.
[31] S. Y. Wong and J. Li, "Enhancing efficiency in photovoltaic hydrogen production: A comparative analysis of MPPT and electrolysis control strategies," *MethodsX*, vol. 14, p. 103220, Jun. 2025, doi: 10.1016/j.mex.2025.103220.

BIOGRAPHIES OF AUTHORS



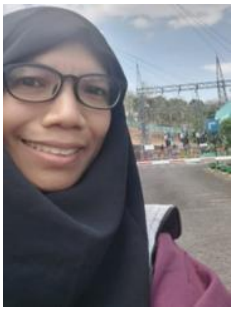
Ahmad Rosyid Idris received the bachelor degree in Electrical Engineering from Hasanuddin University, Makassar, Indonesia, in 2008, and the master degree in Electrical Engineering from Hasanuddin University, Makassar, Indonesia, in 2010. He is currently a lecturer at the Department of Electrical Engineering, Politeknik Negeri Ujung Pandang, Makassar, Indonesia and a member of the Solar Energy System Research Group (SESRG). His teaching and research interests include electrical power systems, renewable energy systems, power electronics, photovoltaic technology, and hydrogen-based energy conversion. He has authored and co-authored several journal articles and conference papers in the field of power engineering and renewable energy systems. He can be contacted at email: ahmadrosyid@poliupg.ac.id.



Faizal Arya Samman is a professor in the Department of Electrical Engineering, at Hasanuddin University, Indonesia. He received bachelor of engineering degree in electrical engineering from Gadjah Mada University, Indonesia, in 1999 and master of engineering degree from Bandung Institute of Technology with a scholarship award from the Indonesian Ministry of National Education, in 2002. He received his Ph.D. degree from Technische Universität Darmstadt, Germany with a scholarship award from Deutscher Akademischer Austausch-Dienst (DAAD, German Academic Exchange Service), in 2010. He worked toward the postdoctoral research in LOEWE-Zentrum adaptronik-research, innovation, application (AdRIA) within the research cooperation framework between Technische Universität Darmstadt and Fraunhofer Institute LBF in Darmstadt, in 2012. His research interests include multiprocessor system-on-chip, computer architecture, analog and digital integrated electronics, power electronics for renewable energy systems and electric vehicles applications, FPGA/CPLD-based digital system design, energy harvesting, and internet of things. He is a member of the IEEE. He can be contacted at email: faizalas@unhas.ac.id.



Alamsyah Achmad received the diploma degree in Electrical Engineering from Universitas Negeri Makassar, Makassar, Indonesia, in 2011, the bachelor degree in Electrical Engineering Education from Universitas Negeri Makassar, Makassar, in 2012, and the master degree in Electrical Power Systems from the Institut Teknologi Sepuluh Nopember, Surabaya, Indonesia, in 2015. He is currently a lecturer at the Department of Electrical Engineering, Diploma-4 Teknik Listrik, Politeknik Negeri Ujung Pandang, Makassar, Indonesia. He is also a member of the Solar Energy System Research Group (SESRG). His research interests include renewable energy systems and artificial intelligence applications in electrical power systems. He is the author and co-author of several journal articles, conference papers, and academic books in the field of power electronics. He can be contacted at email: alamsyahachmad@poliupg.ac.id.



Ir. Musfirah Putri Lukman, S.T., M.T., M.Sc. earned her bachelor of engineering (S.T.) degree in Electrical Engineering from Hasanuddin University, Indonesia, in 2006, and subsequently obtained her professional engineering qualification (Ir.) in applied engineering. She completed her graduate studies through a dual-degree program jointly conducted by Hasanuddin University and Kyushu University, Japan. Under this scheme, she pursued one year of advanced coursework and research at Hasanuddin University, leading to the master of engineering (M.T.) degree, and subsequently spent one year at Kyushu University, where she completed the requirements for the master of science (M.Sc.) degree in 2012. Her academic and research interests include electrical power systems, intelligent control, IoT-based monitoring, automation systems, and interdisciplinary integration between electrical engineering and informatics. She has contributed to various research publications, academic activities, and collaborative technology development projects. She can be contacted at email: musfirahputrilukman@poliupg.ac.id.



Dr. Syamsumarlin Taha, A.Md., S.Pd., M.Pd., earned an associate degree in Electrical Engineering from Makassar State University in 2007, a bachelor of Education degree from Makassar State University in 2009, a master of Science in Vocational Technology Education from the Postgraduate Program from Makassar State University in 2013, a doctor of Science in Education from the Postgraduate Program from Makassar State University, Indonesia. Currently, he is a lecturer in the Department of Electrical Engineering, Faculty of Engineering and Informatics, Patria Artha University, Gowa, Indonesia, and also one of the competency assessors in the Electric Power Distribution Sector. His teaching and research interests include regulation and standardization of electricity, electricity safety (K2), electrical installations, protection, and grounding. He has written and co-authored a book entitled "Marlin Model Learning to Improve Electrical Safety," and several book chapters, references published by the Indonesian Writers' Group, as well as several journal articles and conference papers in the field of electrical installations and safety. He can be contacted at email: syamsumarlintaha@gmail.com.